Grouped Sequency-arranged Rotation: Optimizing Rotation Transformation for Quantization for Free

Euntae Choi[*], **Sumin Song**[*], **Woosang Lim**[*], **Sungjoo Yoo**
Seoul National University
euntae.choi175@gmail.com, songsm921@snu.ac.kr,
ftyg656512@snu.ac.kr, sungjoo.yoo@gmail.com

Abstract

Large Language Models (LLMs) face deployment challenges due to high computational costs, and while Post-Training Quantization (PTQ) offers a solution, existing rotation-based methods struggle at very low bit-widths like 2-bit. We introduce a novel, training-free approach to construct an improved rotation matrix, addressing the limitations of current methods. The key contributions include leveraging the Walsh-Hadamard transform with sequency ordering, which clusters similar frequency components to reduce quantization error compared to standard Hadamard matrices, significantly improving performance. Furthermore, we propose a Grouped Sequency-arranged Rotation (GSR) using block-diagonal matrices with smaller Walsh blocks, effectively isolating outlier impacts and achieving performance comparable to optimization-based methods without requiring any training. Our method demonstrates robust performance on reasoning tasks and Perplexity (PPL) score on WikiText-2. Our method also enhances results even when applied over existing learned rotation techniques.

1 Introduction

Large Language Models (LLMs), despite their widespread success, face deployment challenges due to high computational costs, particularly in resource-constrained settings. Quantization, which reduces the numerical precision of model parameters, offers a viable solution by decreasing model size and accelerating computation with minimal accuracy loss. Post-Training Quantization (PTQ) is especially attractive as it avoids costly retraining.

Within PTQ for LLMs, rotation-based methods like QuaRot (Ashkboos et al., 2024) are common but suffer severe performance degradation at low bit-widths, such as 2-bit weight quantization

(W2), exhibiting high Perplexity (PPL) of 20.29 on WikiText-2 (Merity et al., 2017). Subsequent methods like SpinQuant (Liu et al., 2025) (PPL of 16.45) and OSTQuant (Hu et al., 2025) (PPL of 10.97) improve accuracy using learnable rotation or scaling matrices, but require additional optimization phases, diminishing the core benefit of PTQ.

To address this, we propose a novel, training-free approach to construct an improved rotation matrix for LLM quantization. Our method leverages the Walsh matrix by rearranging the rows of the Hadamard matrix so that the sequency is sorted in ascending order. This clusters similar frequency components, reducing intra-group variance and quantization error compared to the standard Hadamard matrix used in QuaRot, improving PPL to 15.38.

Furthermore, inspired by local rotation techniques (Lin et al., 2024; Xiang et al., 2025), we introduce Grouped Sequency-arranged Rotation (GSR). The GSR employs a block-diagonal matrix with smaller Walsh matrices, effectively isolating outlier impacts within each quantization group. This significantly enhances performance, achieving a PPL of 11.59 and an average zero-shot tasks accuracy of 42.44% – comparable to optimization-based methods without requiring training. Our approach also improves when applied to existing learning-based methods like SpinQuant and OSTQuant.

2 Preliminaries

2.1 Walsh-Hadamard Transform and Sequency

A Hadamard matrix with a size of a non-negative power of two is usually constructed by Sylvester's method as follows:

$$\mathbf{H}_2 = \frac{1}{\sqrt{2}} \begin{bmatrix} 1 & 1 \\ 1 & -1 \end{bmatrix} \quad \text{and} \quad \mathbf{H}_{2^n} = \mathbf{H}_2 \otimes \mathbf{H}_{2^{n-1}}. \tag{1}$$

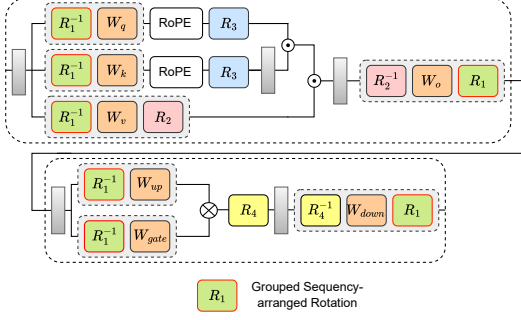[*]these authors contributed equally.

Figure 1: Overall diagram of rotation scheme. We applied Grouped Sequency-arranged Rotation (GSR) on R_1.

A Walsh matrix is derived by applying the bit-reversal and the Gray-code permutation to the Hadamard matrix (Tam and Goulet, 1972).

Sequency is the number of sign flips in a row of such matrices. The Walsh matrix follows sequency ordering where the sign flips of each row are arranged in ascending order. In contrast, the Hadamard matrix is in natural ordering, where the sequency value of the i-th row is defined as follows:

$$S(i) = \text{bit\_count}(i \oplus (i >> 1)). \quad (2)$$

For instance, the rows of a Hadamard matrix of size 8 have 0, 7, 3, 4, 1, 6, 2, and 5 sequency values.

Such matrices serve as a transform by themselves, and we call each row (or column) a sequency filter.

2.2 Rotation for LLM Quantization

Since a Hadamard matrix can be used as a rotation matrix when scaled and has an efficient algorithm, recent state-of-the-art methods make extensive use of the Hadamard transform (Ashkboos et al., 2024; Xiang et al., 2025; Lin et al., 2024; Liu et al., 2025; Hu et al., 2025). We followed SpinQuant's terminology to describe our rotation scheme as Fig. 1. At Fig. 1, R_1 rotates all hidden activations between transformer blocks, R_2 rotates the value activation, R_3 rotates the query and key activations after RoPE, and R_4 rotates the input activation of the down projection. Specifically for R_1, a Randomized Hadamard Transform (RHT) is employed following the proposition in Quip# (Tseng et al., 2024) for better incoherence processing. This way, the outliers in the activation distribution are largely suppressed, achieving deployable W4A4KV4[1] performance on famous LLM models.

---

[1] We notate x-bit weight, y-bit activation, z-bit KV-cache into WxAyKVz like W4A4KV4.

3 Methodology

3.1 Grouped Sequency-arranged Rotation

We propose Grouped Sequency-arranged Rotation (GSR), a training-free rotation technique to improve post-training quantization of LLMs under extreme quantization settings such as W2 and W2A4[2]. We denote the input and output channels of a weight $W \in \mathbb{R}^{C \times H}$ with C and H. G and N denote the group size and the number of groups, respectively, so that $C = NG$.

As exhibited in Fig. 1, we design a signal processing-inspired rotation matrix that can independently be plugged into existing rotation-based PTQ algorithms, as follows:

$$R_{GSR} = \begin{bmatrix} H_{wal} & \mathbf{0} & \cdots & \cdots & \mathbf{0} \\ \mathbf{0} & H_{wal} & \mathbf{0} & \cdots & \vdots \\ \vdots & \mathbf{0} & \ddots & \mathbf{0} & \vdots \\ \vdots & \vdots & \mathbf{0} & \ddots & \mathbf{0} \\ \mathbf{0} & \cdots & \cdots & \mathbf{0} & H_{wal} \end{bmatrix} \quad (3)$$

, where $H_{wal} \in \{-1, 1\}^{G \times G}$ is a $G \times G$ Walsh matrix, with G being the quantization group size, and $\mathbf{0}$ is a $G \times G$ zero matrix.

The proposed R_{GSR} has several advantages over the RHT and the SpinQuant matrices: First, like QuaRot (Ashkboos et al., 2024), it can replace any rotation matrix in existing PTQ methods without training for virtually free, as the only additional operation required is to pre-process a Sylvester-constructed Hadamard matrix to a Walsh matrix and apply the Kronecker product with an identity matrix before going into quantization. Second, it can systematically reduce weight quantization error by strategically arranging sequency filters with similar yet diverse sequency values (Section 3.2). Third, it can also serve as an enhanced initialization for training-based methods such as SpinQuant (Liu et al., 2025) and OSTQuant (Hu et al., 2025) (Section 4).

3.2 The Effect of Sequency Arrangement on Group Quantization

To justify our design, we investigate how the sequency ordering in our GSR can improve group quantization on weights. As shown in Fig. 1, the weights are rotated twice as follows:

$$W' = R_f^{-1} W R_r, \quad (4)$$

---

[2] Since 2-bit per-channel quantization can easily fail to converge, we assume group quantization in all cases.

where R_f and R_r are rotation matrices applied to the front and rear side of a weight W, respectively. For query weight W_q as an example, $R_f = R_1$ and $R_r = I$ hold. We do not consider local rotation in this section for brevity.

An (i, j) element of the rotated weight $(W'[i, j])$ can be expressed as follows:

$$
\begin{aligned}
W'[i,j] &= \langle (R_f^{-1}W)[i,:], R_r[:,j] \rangle \\
&= \Big\langle \Big[\langle R_f^{-1}[i,:], W[:,1] \rangle, \langle R_f^{-1}[i,:], W[:,2] \rangle, \\
&\qquad \ldots, \langle R_f^{-1}[i,:], W[:,H] \rangle \Big], R_r[:,j] \Big\rangle .
\end{aligned}
\tag{5}
$$

An n-th row group in W' can be expressed as $W'[nG : (n+1)G, :]$, which leads to our observation #1 by simply substituting i to $nG : (n+1)G$ in Eqn. 5.

> **Observation #1**
>
> Under group quantization, each column group in the front rotation matrix R_f generates distinct rotated weight groups, and all columns in the rear rotation matrix R_r are always applied to all rows in the original weight.
>
> In other words, a group in the rotated weight W' is the original weight transformed by the corresponding group of filters in the front rotation matrix and then by all filters in the rear rotation matrix.

Comparing Hadamard and Walsh Now, we relate the sequency arrangement to group quantization performance. For R_r, the arrangement has no impact as long as the set of sequency values is equal, which is the case with comparing the Hadamard and Walsh matrices. Therefore, we focus on R_f. The Walsh matrix (with the sequency ordering) has smaller sequency variance within each column group than the Hadamard matrix because the sequency values increase linearly. Since sequency is analogous to frequency in the conventional frequency-domain filtering, the Walsh matrix will produce rotated weight groups with fewer massive outliers. As shown in Table 1, R_1 works as R_f on many different types of transformer weights including W_q, W_k, W_v, W_{up}, and W_{gate}, changing R_1 from Hadamard to Walsh helps reduce the quantization error for these weights.

Comparing RHT and Walsh The randomization method in Quip# (Tseng et al., 2024) and

| Weight	W_q	W_k	W_v	W_o	W_{up}	W_{gate}	W_{down}
R_f	R_1	R_1	R_1	R_2	R_1	R_1	R_4
R_r	I	I	R_2	R_1	I	I	R_1

Table 1: Rotation matrix configuration on each weight type in LLaMA-like transformer architecture. I is the identity matrix.

QuaRot (Ashkboos et al., 2024) only flips the signs of diagonal elements in a Hadamard matrix. This process keeps the overall sequency arrangement with no significant changes. Therefore, we can compare the RHT against the Walsh following the same logic as in the previous section.

3.3   Global vs. Local Rotation
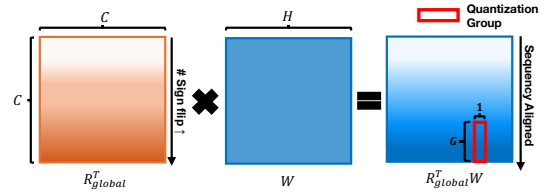
(a) Global rotation applies a full-matrix transformation across all dimensions and spreads outlier effects widely.
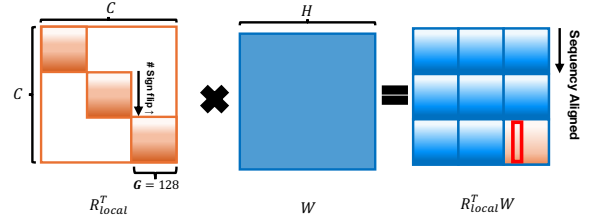
(b) Local rotation applies block-diagonal transformations within groups and confines outlier effects within each block. For illustration purposes, three blocks are depicted, while the actual number of blocks is given by $N = C/G$.

Figure 2: Overview of global and local rotation strategies. Global rotation transforms the entire space and amplifies outlier effects and local rotation advances control over outliers within blocks to improve quantization robustness.

Local rotation (using block-diagonal matrices) is generally more effective than global rotation (using a single large matrix) (Lin et al., 2024; Xiang et al., 2025; Xiang and Zhang, 2024). Global rotation can struggle to effectively handle outliers, whether in activations or weights, as it spreads their impact to the whole input channel. Local rotation, however, confines the effects of such outliers within their specific block or group as in Fig. 2 (b). When used with the Walsh matrix, this containment helps better reduce errors, which is also beneficial for low-bit weight quantization.

Method	Bits	R_1	PPL↓	0-shot↑	Method	Bits	R_1	PPL↓	0-shot↑	Method	Bits	R_1	PPL↓	0-shot↑
	W16A16		5.47	69.81		W16A16		5.47	69.81		W16A16		5.47	65.21
QuaRot	W2A16	GH	20.29	32.06	SpinQuant	W2A16	GH	16.45	31.04	OSTQuant	W2A16	GH	10.97	45.52
		GW	**15.38**	**39.30**			GW	16.44	34.52			GW	**9.51**	**46.83**
		LH	12.11	41.01			LH	13.17	39.84			LH	9.16	49.84
		GSR	**11.59**	**42.44**			GSR	12.04	42.11			GSR	**9.03**	**50.51**
QuaRot	W2A4	GH	31.33	27.87	SpinQuant	W2A4	GH	22.94	31.77	OSTQuant	W2A4	GH	16.16	38.18
		GW	**20.34**	**33.75**			GW	**18.86**	**32.05**			GW	14.68	40.67
		LH	17.74	36.88			LH	15.79	34.57			LH	12.44	43.69
		GSR	**15.23**	**37.89**			GSR	15.47	**34.75**			GSR	**11.77**	**44.56**

Table 2: Comparison of the perplexity score on WikiText-2 and the averaged accuracy on zero-shot common-sense reasoning tasks. This experiment presents a comparative analysis across different methods to elucidate the performance differences arising from the types of rotation matrices employed. In the R_1 column, the notations "G", "L", and "H" correspond to global, local, and Hadamard, respectively. For example, 'GH' indicates that a global Hadamard rotation is applied to R_1.

4 Experimental Results

Baseline We conducted experiments to assess whether the proposed GSR offers improved performance over previously used rotation matrices. Comparisons were made across QuaRot, SpinQuant, and OSTQuant. To ensure a fair evaluation, all methods were assessed by applying group quantization to their originally reported quantization configurations, under W2A16 and W2A4 settings. Changes in rotation, such as switching to the Walsh matrix or applying local rotation, were applied only to R_1, as further analyzed in the Appendix A.2. Details of the quantization configurations are provided in the Appendix A.1.

Model and Datasets The proposed method was evaluated on Llama-2-7B (Touvron et al., 2023). To assess general language modeling capability, we measured PPL on WikiText-2 (Merity et al., 2017) with a context length of 2048 tokens. To evaluate reasoning ability, we conducted common zero-shot evaluations on a set of reasoning tasks, following the same datasets used in baseline methods. Specifically, QuaRot and SpinQuant were evaluated on Arc (Easy and Challenge) (Clark et al., 2018), HellaSwag (Zellers et al., 2019), LAMBADA (Paperno et al., 2016), PIQA (Bisk et al., 2020), and Wino-Grande (Sakaguchi et al., 2021), while OSTQuant was additionally evaluated on BoolQ (Clark et al., 2019), OpenBookQA (Mihaylov et al., 2018), and SIQA (Sap et al., 2019).

Implementation Details and Overall Results We denote the global Hadamard matrix as GH, the global Walsh matrix as GW, local Hadamard matrix as LH. All Hadamard matrices are randomized, following common practice in previous rotation-based algorithms. When constructing Walsh matrices, the original Hadamard matrix is used. The other details not mentioned here are listed in the Appendix A.1.

The overall results are summarized in Table 2. Across all methods, our proposed approach consistently outperforms the GH, achieving lower PPL and higher accuracy on reasoning tasks. In particular, applying the GW to QuaRot (i.e., re-ordering rows of the Hadamard matrix with natural ordering) yields approximately 1 point lower PPL compared to SpinQuant, validating the benefit of the sequency arrangement. Given that SpinQuant typically consumes much greater computational costs than QuaRot, this result suggests that adopting GSR enables QuaRot to achieve superior performance and efficiency. While OSTQuant learns both the rotation matrix and the smooth factor through optimization and achieves a PPL of 10.97 in the W2 setting, QuaRot with GSR attains a comparable PPL of 11.59 by simply replacing R_1 in a training-free manner. In the W2A4 setting, QuaRot with GSR even surpasses OSTQuant, achieving a lower PPL of 15.23 compared to 16.16, indicating that better performance can be obtained with fewer resources. The effectiveness of GSR also holds when applied to OSTQuant, consistently leading to further performance gains.

The advantage of the sequence arrangement is enhanced when paired with the local rotation. When comparing the LH and GSR on QuaRot, GSR consistently also delivers better performance across all cases, similar to the improvements observed in global rotation (GH vs GW). Moreover, in zero-shot task evaluations, the Walsh matirx con-

sistently outperforms the Hadamard. Notably, in the QuaRot W2 setting, the GW achieves approximately 7 points higher accuracy compared to the GH, again surpassing SpinQuant. Complete individual scores for each task are provided in Appendix A.3.

5 Conclusion

In this paper, we proposed a novel training-free rotation technique, Grouped Sequency-arranged Rotation (GSR), inspired by signal processing theory on Walsh-Hadamard transform and sequency. The GSR makes use of the Walsh matrix to place transformed weights filtered by similar sequency values closer, and combines the local rotation idea for constraining possible remaining outliers within a single quantization group per row. A theoretical justification is also provided for each component. Experimental results verify the effectiveness of our proposed method on common benchmarks for LLM quantization, including WikiText-2 and popular zero-shot common-sense reasoning tasks.

Limitations

Our proposed method has proven effective only under extremely low-bit weight quantization with group quantization. On larger bit configurations, the quantization error becomes much less significant, so that the sequency alignment cannot show visible improvement. In addition, to ensure the generalizability of our approach, we plan to extend our experiments to other model architectures and datasets in future work.

References

Saleh Ashkboos, Amirkeivan Mohtashami, Maximilian L Croci, Bo Li, Martin Jaggi, Dan Alistarh, Torsten Hoefler, and James Hensman. 2024. Quarot: Outlier-free 4-bit inference in rotated llms. In *Thirty-eighth Conference on Neural Information Processing Systems*.

Yonatan Bisk, Rowan Zellers, Jianfeng Gao, Yejin Choi, and 1 others. 2020. Piqa: Reasoning about physical commonsense in natural language. In *Proceedings of the AAAI conference on artificial intelligence*, volume 34, pages 7432–7439.

Christopher Clark, Kenton Lee, Ming-Wei Chang, Tom Kwiatkowski, Michael Collins, and Kristina Toutanova. 2019. BoolQ: Exploring the surprising difficulty of natural yes/no questions. In *Proceedings of the 2019 Conference of the North American Chapter of the Association for Computational Linguistics:*

Human Language Technologies, Volume 1 (Long and Short Papers), pages 2924–2936, Minneapolis, Minnesota. Association for Computational Linguistics.

Peter Clark, Isaac Cowhey, Oren Etzioni, Tushar Khot, Ashish Sabharwal, Carissa Schoenick, and Oyvind Tafjord. 2018. Think you have solved question answering? try arc, the ai2 reasoning challenge. *arXiv:1803.05457v1*.

Elias Frantar, Saleh Ashkboos, Torsten Hoefler, and Dan Alistarh. 2022. Optq: Accurate quantization for generative pre-trained transformers. In *The Eleventh International Conference on Learning Representations*.

Xing Hu, Yuan Cheng, Dawei Yang, Zhixuan Chen, Zukang Xu, JiangyongYu, XUCHEN, Zhihang Yuan, Zhe jiang, and Sifan Zhou. 2025. OSTQuant: Refining large language model quantization with orthogonal and scaling transformations for better distribution fitting. In *The Thirteenth International Conference on Learning Representations*.

Haokun Lin, Haobo Xu, Yichen Wu, Jingzhi Cui, Yingtao Zhang, Linzhan Mou, Linqi Song, Zhenan Sun, and Ying Wei. 2024. Duquant: Distributing outliers via dual transformation makes stronger quantized llms. *Advances in Neural Information Processing Systems*, 37:87766–87800.

Zechun Liu, Changsheng Zhao, Igor Fedorov, Bilge Soran, Dhruv Choudhary, Raghuraman Krishnamoorthi, Vikas Chandra, Yuandong Tian, and Tijmen Blankevoort. 2025. Spinquant: Llm quantization with learned rotations. In *The Thirteenth International Conference on Learning Representations*.

Stephen Merity, Caiming Xiong, James Bradbury, and Richard Socher. 2017. Pointer sentinel mixture models. In *International Conference on Learning Representations*.

Todor Mihaylov, Peter Clark, Tushar Khot, and Ashish Sabharwal. 2018. Can a suit of armor conduct electricity? a new dataset for open book question answering. In *Proceedings of the 2018 Conference on Empirical Methods in Natural Language Processing*, pages 2381–2391, Brussels, Belgium. Association for Computational Linguistics.

Denis Paperno, Germán Kruszewski, Angeliki Lazaridou, Ngoc Quan Pham, Raffaella Bernardi, Sandro Pezzelle, Marco Baroni, Gemma Boleda, and Raquel Fernández. 2016. The LAMBADA dataset: Word prediction requiring a broad discourse context. In *Proceedings of the 54th Annual Meeting of the Association for Computational Linguistics (Volume 1: Long Papers)*, pages 1525–1534, Berlin, Germany. Association for Computational Linguistics.

Keisuke Sakaguchi, Ronan Le Bras, Chandra Bhagavatula, and Yejin Choi. 2021. Winogrande: An adversarial winograd schema challenge at scale. *Communications of the ACM*, 64(9):99–106.

Maarten Sap, Hannah Rashkin, Derek Chen, Ronan Le Bras, and Yejin Choi. 2019. Social IQa: Commonsense reasoning about social interactions. In *Proceedings of the 2019 Conference on Empirical Methods in Natural Language Processing and the 9th International Joint Conference on Natural Language Processing (EMNLP-IJCNLP)*, pages 4463–4473, Hong Kong, China. Association for Computational Linguistics.

Le Dinh Chon Tam and R.Y. Goulet. 1972. On arithmetical shift for walsh functions. *IEEE Transactions on Computers*, C-21(12):1451–1452.

Hugo Touvron, Louis Martin, Kevin Stone, Peter Albert, Amjad Almahairi, Yasmine Babaei, Nikolay Bashlykov, Soumya Batra, Prajjwal Bhargava, Shruti Bhosale, and 1 others. 2023. Llama 2: Open foundation and fine-tuned chat models. *arXiv preprint arXiv:2307.09288*.

Albert Tseng, Jerry Chee, Qingyao Sun, Volodymyr Kuleshov, and Christopher De Sa. 2024. QuIP$\#$: Even better LLM quantization with hadamard incoherence and lattice codebooks. In *Forty-first International Conference on Machine Learning*.

Jingyang Xiang and Sai Qian Zhang. 2024. Dfrot: Achieving outlier-free and massive activation-free for rotated llms with refined rotation. *arXiv preprint arXiv:2412.00648*.

Jingyang Xiang, Ying Zhang, Chi Ma, Yujie Wang, yulei, LiuChuan, Wei Lin, and Yong Liu. 2025. Duarot: Dual rotation for advanced outlier mitigation in rotated LLMs.

Rowan Zellers, Ari Holtzman, Yonatan Bisk, Ali Farhadi, and Yejin Choi. 2019. HellaSwag: Can a machine really finish your sentence? In *Proceedings of the 57th Annual Meeting of the Association for Computational Linguistics*, pages 4791–4800, Florence, Italy. Association for Computational Linguistics.

A   Appendix

A.1   Additional Implementation Details

For a fair comparison, only group quantization was additionally applied, while the primary quantization settings originally reported for each method were preserved. The detailed settings applied to each method are described below.

GPTQ   During weight quantization with GPTQ (Frantar et al., 2022), the calibration was performed by sampling 128 contexts, each consisting of 2048 tokens, from the WikiText2 dataset.

QuaRot   For QuaRot (Ashkboos et al., 2024), GPTQ-based quantization was applied with asymmetric weight quantization, MSE-based clipping, and group quantization using a group size of 128. Activation quantization was performed using symmetric round-to-nearest (RTN) quantization with a clipping ratio of 0.9 and a group size of 128.

SpinQuant   For SpinQuant (Liu et al., 2025), since GPTQ was used during PTQ, weight quantization was not applied during the rotation matrix training phase. However, when activation quantization was included, activation quantization-aware training was performed using an RTN quantizer, with symmetric quantization and a group size of 128 applied to activations.

OSTQuant   For OSTQuant (Hu et al., 2025), both the rotation matrix and the smoothing factor were learned. During weight-only quantization, weight-quantization-aware training was conducted using asymmetric quantization, MSE-based clipping, and a group size of 128. When quantizing both weights and activations, the weights were kept frozen, and only the effect of activation RTN quantization was considered, with a group size of 128 applied.

A.2   Ablation Study

Method	R_1	R_4	**PPL**	**PPL**†
QuaRot	LH	GH	12.11	17.74
	LH	LH	12.65	14.64
	GSR	GH	11.59	15.23
	GSR	LH	11.22	13.83

Table 3: Ablation results on the effect of local rotation for R_4 in Llama-2-7B. PPL represents the results for W2, and PPL† represents the results for W2A4.

Global and Local Rotation on R_4   As part of the ablation study, we applied local rotation to R_4, originally using global rotation. Table 3 shows that local rotation consistently improves performance under activation quantization (W2A4), but has negligible impact under weight-only quantization (W2).

Given the role and placement of R_4, it primarily rotates activation outliers through an online rotation mechanism before input activations enter the down-projection of the FFN layer. From the weight perspective, since R_1 and R_4 are fused into the weights during inference, the benefit of local rotation is realized only once. Thus, the performance gains observed from modifications to R_4 can be

attributed mainly to the activation quantization process.

Nonetheless, applying local rotation to the online rotation introduces practical challenges. In particular, it disables the use of the fast-hadamard-transform, requiring the entire FP32 matrix tensor to be stored in memory during inference, which is impractical. We left addressing this limitation for future work.

A.3 Complete Reasoning Tasks Results

In this section, Table 4 and Table 5 present evaluation results for each zero-shot task.

#Bits	Method	R_1	ARC-c	ARC-e	Hella.	lambada	lambada-o	lambada-s	PIQA	Wino.	Avg.
16-16			46.25	74.58	75.99	71.12	73.92	68.33	79.11	69.14	69.81
2-16	QuaRot	GH	23.04	43.27	35.51	13.33	14.48	12.19	59.14	55.49	32.06
		GW	25.94	44.49	42.07	27.88	30.53	25.23	61.26	56.99	39.30
		LH	27.22	48.91	46.12	27.56	30.18	24.94	66.38	56.75	41.01
		GSR	26.79	49.71	47.86	30.90	35.46	26.35	64.85	57.62	42.44
2-4	QuaRot	GH	21.67	35.31	33.00	8.64	9.72	7.55	57.13	49.96	27.87
		GW	22.78	38.34	36.56	19.75	22.49	17.00	58.81	54.30	33.75
		LH	25.77	43.94	41.20	22.52	23.95	21.09	62.62	53.91	36.88
		GSR	27.22	45.20	43.46	23.83	26.92	20.75	61.64	54.14	37.89
2-16	SpinQuant	GH	22.70	41.29	34.37	12.65	14.26	11.04	57.83	54.14	31.04
		GW	22.70	40.82	36.57	20.98	21.41	20.55	59.19	53.91	34.52
		LH	25.43	45.58	42.43	28.58	31.34	25.81	63.17	56.35	39.84
		GSR	25.34	46.46	44.90	32.73	34.95	30.51	64.31	57.70	42.11
2-4	SpinQuant	GH	24.23	38.97	34.68	14.36	15.74	12.98	57.13	56.04	31.77
		GW	22.78	37.04	33.75	17.70	20.32	15.08	57.13	52.57	32.05
		LH	23.89	40.28	39.80	19.25	21.08	17.43	60.61	54.22	34.57
		GSR	25.17	41.58	36.54	20.68	23.21	18.14	59.74	52.96	34.75

Table 4: Complete comparison of accuracy on Zero-shot Common Sense Reasoning tasks for Llama2-7B with QuaRot and SpinQuant. **lambada-o** and **lambada-s** represent **lambada-openai** and **lambada-standard**, respectively.

#Bits	Method	R_1	ARC-c	ARC-e	boolq	Hella.	lambada-o	openbook-qa	PIQA	Social-IQA	Wino.	Avg.
16-16			46.42	74.33	77.71	75.94	73.69	44.20	79.16	45.91	69.53	65.21
2-16	OSTQuant	GH	23.63	50.38	62.87	34.75	40.19	19.60	63.44	36.85	59.04	45.52
		GW	25.00	53.79	63.15	36.16	39.14	19.80	65.61	38.33	59.43	46.83
		LH	27.56	57.53	63.30	39.47	50.96	20.00	66.76	39.36	59.98	49.84
		GSR	26.62	60.56	65.29	38.69	56.20	22.40	66.54	38.08	61.09	50.51
2-4	OSTQuant	GH	19.37	39.14	50.98	31.48	18.38	15.20	60.39	36.08	53.28	38.18
		GW	19.88	45.08	61.83	32.00	22.61	15.00	60.23	36.34	52.09	40.67
		LH	24.66	50.25	63.21	34.82	26.61	18.60	63.93	36.80	55.33	43.69
		GSR	23.21	51.89	62.81	35.05	33.75	18.40	63.28	37.72	56.59	44.56

Table 5: Complete comparison of accuracy on Zero-shot Common Sense Reasoning tasks for Llama2-7B with OSTQuant. **lambada-o** represents **lambada-openai**.